Appl Phys B (2010) 98: 261–265
DOI 10.1007/s00340-009-3842-z

Applied Physics B
Lasers and Optics

RAPID COMMUNICATION

Abnormal upconversion luminescence from Yb^{3+} doped and Tb^{3+}/Yb^{3+} codoped high silica glasses induced by intrinsic optical bistability

Q. Zhang · G. Chen · Y. Xu · X. Liu · B. Qian · G. Dong · Q. Zhou · J. Qiu · D. Chen

Received: 11 August 2009 / Revised version: 9 October 2009 / Published online: 10 December 2009

Abstract Upconversion luminescence (UCL) properties from Yb^{3+} doped and Tb^{3+}/Yb^{3+} codoped high silica glasses excited by a 980 nm laser diode are investigated. The ln–ln plots of the UCL intensity versus laser power show abnormal relations: the slopes are larger than those reported in other papers. When tuning the laser power up and down successively, intrinsic optical bistability of Yb^{3+} ions is observed at room temperature in the visible and infrared range without external cavity. And this nonlinear effect induces the abnormal UCL phenomena.

1 Introduction

Intensive research has recently been dedicated to obtain laser radiation in the visible spectrum. Upconversion luminescence (UCL) in rare-earth (RE) doped materials can be an efficient mechanism to obtain visible (VIS) and near-infrared (NIR) laser radiation. The UCL process in Tb^{3+} doped glasses, crystal and fibers is an important route to obtain green radiation [1–7]. Hosts adopted in UCL research are mainly fluoride and phosphate crystal and glass. On the other hand, high silica glass (HSG) has advantages such as higher chemical stability and better mechanical properties, but it is difficult to generate UCL due to their high phonon energies. In Tb^{3+}/Yb^{3+} codoped materials, the UC efficiency is also determined by the energy transfer between Tb^{3+} and Yb^{3+} ions. The sensitization of Tb^{3+} by Yb^{3+} ions is usually expressed in terms of a dipole-dipole interaction and follows an R^{-6} dependence (R is the average distance between Tb^{3+} and Yb^{3+} ions). So the enhancement of the energy transfer efficiency from Yb^{3+} to Tb^{3+} can be realized by shortening R. It will also enhance the UCL of Tb^{3+}. Nanoporous glasses are apt to accommodate more doped RE ions with the smaller inter-distance after hav-

Q. Zhang · X. Liu · B. Qian · G. Dong · Q. Zhou · D. Chen (✉)
Key Laboratory of Material Science and Technology for High Power Lasers, Shanghai Institute of Optics and Fine Mechanics, Chinese Academy of Sciences, No. 390 Qinghe Road, Jiading, Shanghai 201800, People's Republic of China
e-mail: d-chen@mail.siom.ac.cn

Q. Zhang
e-mail: qiangzhang_china@126.com

X. Liu
e-mail: lxf_lxf@126.com

B. Qian
e-mail: qianbin1984@sina.com

G. Dong
e-mail: guoping_dong@163.com

Q. Zhou
e-mail: kerryqling@hotmail.com

Q. Zhang · X. Liu · B. Qian · G. Dong
Graduate School of the Chinese Academy of Sciences, Beijing 100039, People's Republic of China

G. Chen · Y. Xu
Key Laboratory for Ultrafine Materials of Ministry of Education, School of Materials Science and Engineering, East China University of Science and Technology, No. 130 Meilong Road, Minhang, Shanghai 200237, People's Republic of China

G. Chen
e-mail: grchen@ecust.edu.cn

Y. Xu
e-mail: yinshengxu@126.com

J. Qiu
State Key Laboratory of Silicon Materials, Zhejiang University, No. 148 Tianmushang Road, Hangzhou 310027, People's Republic of China
e-mail: qjr@zju.edu.cn

ing been sintered. In this paper, we present our latest work on UCL behavior of Yb^{3+} doped HSG and $Tb3^{+}/Yb^{3+}$ codoped HSG. Intense glaucous and green emissions occur when the samples are excited by 980 nm laser diode and the UCL shows abnormal relations between laser power and UCL intensity. We observe for the first time intrinsic optical bistability (IOB) of Yb^{3+} at room temperature without external cavity and make explicit the relation of the abnormal relations and IOB.

2 Experimental

The porous glass is fabricated by removing the borate phase from phase-separated alkali-borosilicate glass in hot acid solution. The composition of the porous glass obtained is $97.0SiO_2 \cdot 2.1B_2O_3 \cdot 0.8Al_2O_3 \cdot 0.1(Na_2O + CaO)$ (wt%). The pores are distributed uniformly in the glass and the porosity is 0.4. The porous glasses are soaked in the 1.0 M HNO_3 solution contained Yb^{3+} or Yb^{3+} and Tb^{3+} ions for 4 hours. The concentrations of Yb^{3+} ions and Tb^{3+} ions in the solution are 0.15 M/L and 0.025 M/L, respectively. Afterwards, the glasses are sintered at 1200°C in air for two hours to obtain Yb^{3+} doped HSG and Tb^{3+}/Yb^{3+} codoped HSG. The concentrations of Yb^{3+} and Tb^{3+} in the HSGes are $6\times10^{19}/cm^3$ and $1 \times 10^{19}/cm^3$ respectively. All of the glass samples are cut to 2 mm × 5 mm × 5 mm for measurements.

An adjustable (0–20 W) Apollo Instruments' laser diode with a central wavelength of 980 nm is used to excite Yb^{3+} doped and Tb^{3+}/Yb^{3+} codoped HSG. The laser beam is focused to about 1 mm on the samples by an optical lens with focal length of 50 mm. Then the UCL and NIR emission spectra are recorded using a Zolix SBP300 spectrofluorometer with a multiplier phototube detector in VIS range and an InGaAs detector in NIR range, respectively.

3 Results and discussions

The UCL spectrum of Tb^{3+} in Tb^{3+}/Yb^{3+} codoped HSGes excited by a 980 nm LD is shown in Fig. 1(a). The spectrum consists of seven emission peaks at 377 nm, 411 nm, 434 nm, 486 nm, 541 nm, 585 nm and 618 nm, which are attributed to the transition of $^5D_3 \to {}^7F_6$,$^5G_6 \to {}^7F_5$,$^5D_3 \to {}^7F_4$, $^5D_4 \to {}^7F_6$, $^5D_4 \to {}^7F_5$, $^5D_4 \to {}^7F_4$ and $^5D_4 \to {}^7F_3$, respectively [3]. As we know, for any process of UCL, the VIS output intensity I_{VIS} is approximately proportional to the power n of NIR excitation intensity I_{NIR}, i.e. $I_{VIS} \propto (I_{NIR})^n$ [2], where n represents the number of photons required to populate the emitting states. The VIS output intensities can be estimated by the integrated intensities of the transition bands. The integrated intensities of the seven bands are calculated by summing the emission intensity in the ranges of 360∼396 nm, 396∼420 nm, 422∼450 nm, 460∼498 nm, 520∼558 nm, 566∼604 nm, 606∼632 nm, respectively. The error of intensity is estimated by measuring the same sample under the same condition for several times and calculating the maximum deviation percent between each other. The error is estimated to be less than 5%. The dependence of UCL emission intensity upon incident pump power is examined and the results are shown as ln–ln plots in Fig. 1(b). The slopes of the aforementioned seven emissions in Tb^{3+}/Yb^{3+} codoped HSG are 4.22, 4.25, 3.98, 3.27, 3.28, 3.33 and 3.24, respectively. It is known from previously reported work that the transitions of $^5D_4 \to {}^7F_J$ ($J = 6$, 5, 4 and 3) usually origins from the energy transfer between Tb^{3+} ions and Yb^{3+} ions, which are attributed to ($2Yb^{3+}$: $^2F_{5/2} \to {}^2F_{7/2}$; Tb^{3+} : $^7F_6 \to {}^5D_4$) with the slope around 2 [1–7]. The Yb^{3+} ions can also transfer its energy to Tb^{3+} ions at $^5D_4$ state where electrons from Tb^{3+} ions are excited to $^5D_3$, $^5G_6$ states, which induces the transition of $^5D_3 \to {}^7F_6$, $^5G_6 \to {}^7F_5$, $^5D_3 \to {}^7F_4$ with the slope about 3 [2]. However, the slopes we obtained in Tb^{3+}/Yb^{3+} codoped HSG are much larger than that in other materials.

Considering the energy transfer from Yb^{3+} ions to Tb^{3+} ions, we also investigate the UCL of Yb^{3+} doped HSG

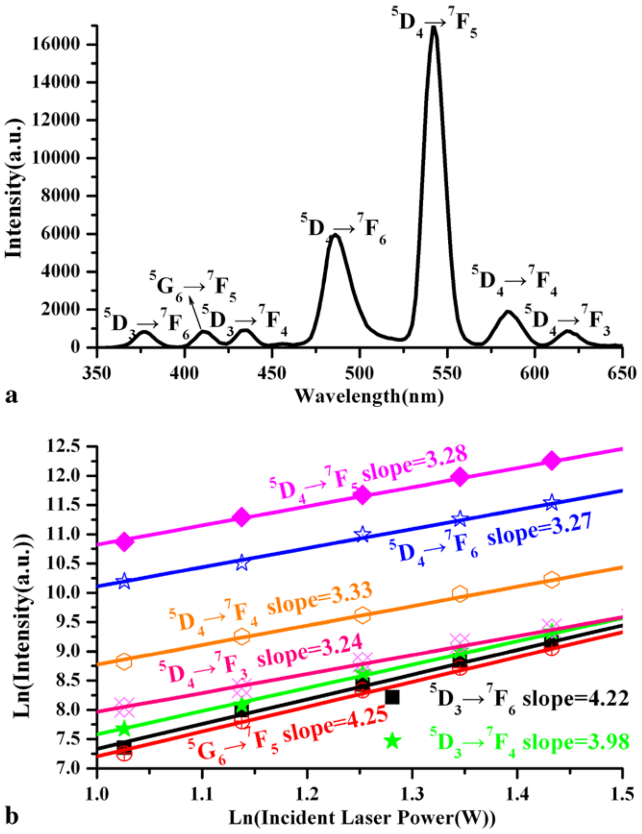

Fig. 1 Upconversion luminescence of Tb^{3+}/Yb^{3+} codoped high silica glass under the excitation of 980 nm laser diode (**a**) and ln–ln plots of the upconversion intensity versus laser power (**b**)

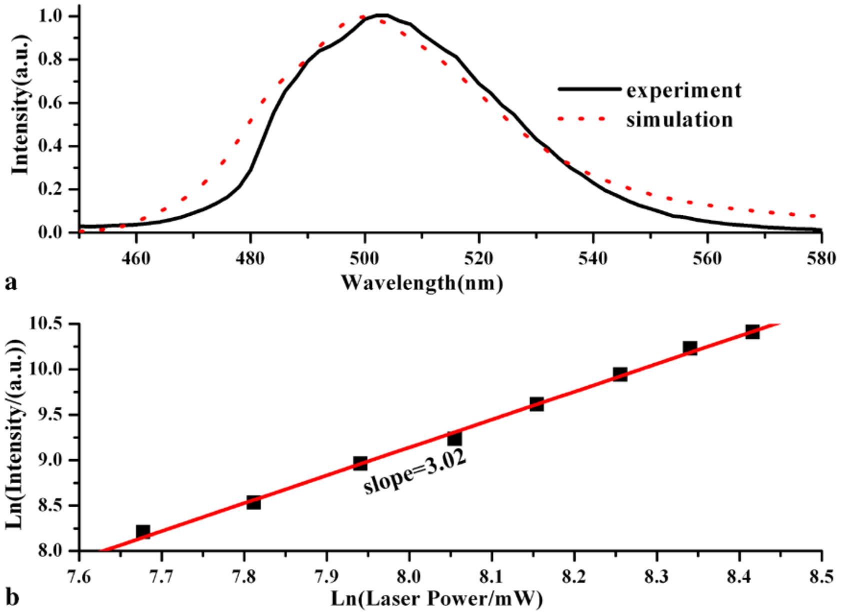

Fig. 2 Upconversion luminescence of Yb^{3+} doped high silica glass under the excitation of 980 nm laser diode (**a**: *black line*), simulation upconversion of Yb^{3+} by self-convoluted (**a**: *red*, *dotted*) and ln–ln plots of the upconversion intensity versus laser power (**b**)

under the excitation of LD as shown in Fig. 2. The integrated range is 450∼580 nm. Figure 2(a) (black, lined) and Fig. 2(b) show the UCL spectrum and ln–ln plot of Yb^{3+} doped HSG, respectively. The Yb^{3+} doped HSG shows broad UCL band centered at about 500 nm; the slope of the ln–ln plots is 3.02. The UCL of Yb^{3+} doped materials is a cooperative process [8–12], which can be described with a self-convoluted NIR emission spectrum since cooperative luminescence comes from the simultaneous de-excitation of two Yb^{3+} ions [12]. So the cooperative UCL spectra of Yb^{3+} in Yb^{3+} doped materials can be calculated by the formula $I_{\mathrm{VIS}}(E)=\int I_{\mathrm{NIR}}(E')I_{\mathrm{NIR}}(E-E')\,\mathrm{d}E'$ [11], where E and E' are the energy of photon, I_{VIS} and I_{NIR} are the emission intensity of Yb^{3+} ions in VIS and NIR range, respectively. The calculated self-convoluted NIR spectrum has been plotted in Fig. 2(a) (red, dotted). By comparison it is found that the emission spectrum of Yb^{3+} doped HSG shows a red shift with emission peak at 502 nm. This peak results from convolution of two peaks at 980 nm and 1030 nm; that is, the intensity of 502 nm emission is correlative to the emission intensity of Yb^{3+} ions at 980 nm and 1030 nm. Therefore, the following relations can be obtained: $I_{\lambda=502\ \mathrm{nm}} \propto I_{\lambda=980\ \mathrm{nm}} \cdot I_{\lambda=1030\ \mathrm{nm}} \propto (I_{\lambda=980\ \mathrm{nm}})^n$, or $I_{\lambda=1030\ \mathrm{nm}} \propto (I_{\lambda=980\ \mathrm{nm}})^{n-1}$, where $I_{\lambda=502\ \mathrm{nm}}$ is the integral intensity centered at 502 nm, $I_{\lambda=980\ \mathrm{nm}}$ and $I_{\lambda=1030\ \mathrm{nm}}$ are integral intensity at 980 nm and 1030 nm, respectively.

For materials with $n \simeq 2$, the relation between $I_{\lambda=1030\ \mathrm{nm}}$ and $I_{\lambda=980\ \mathrm{nm}}$ is linear. But in Yb^{3+} doped HSG with $n=3.02$, $I_{\lambda=1030\ \mathrm{nm}}$ and $I_{\lambda=980\ \mathrm{nm}}$ have a square relation accordingly. The ln–ln relation of $I_{\lambda=1030\ \mathrm{nm}}$ versus laser power has also been plotted in Fig. 3. It is seen from figure that the slope is equal to 1 when the laser power is low and becomes 1.81 when the laser power is high. As the UCL of Yb^{3+} doped HSG could not be observed at low excitation power, we can deduce that the abnormal UCL of Yb^{3+} doped HSG comes from the quasi square relation between $I_{\lambda=1030\ \mathrm{nm}}$ and $I_{\lambda=980\ \mathrm{nm}}$.

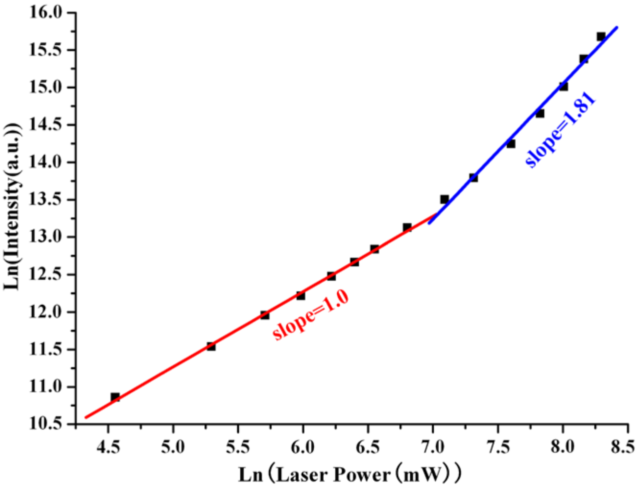

Fig. 3 Ln–ln plots of the upconversion intensity of Yb^{3+} in Yb^{3+} doped high silica glass versus laser power

We also tune the laser power in a larger range to have a clearer understanding of this phenomenon. The luminescence spectra of Yb^{3+} doped HSG in VIS/NIR range versus incident laser power are plotted in Fig. 4. We can see that both luminescence intensities show hysteretic behavior when the laser power is increased and decreased successively. The upward UCL and NIR luminescence measurements are carried out at 2500∼4300 mW (labeled by rectangle in Fig. 4), which locates at the rising part of the hysteretic loop. This hysteretic behavior is the intrinsic optical bistability (IOB) of Yb^{3+} ions in HSG. IOB was

Fig. 4 Luminescence intensity versus laser power of Yb^{3+} doped high silica glass in visible (**a**) and near-infrared (**b**) range

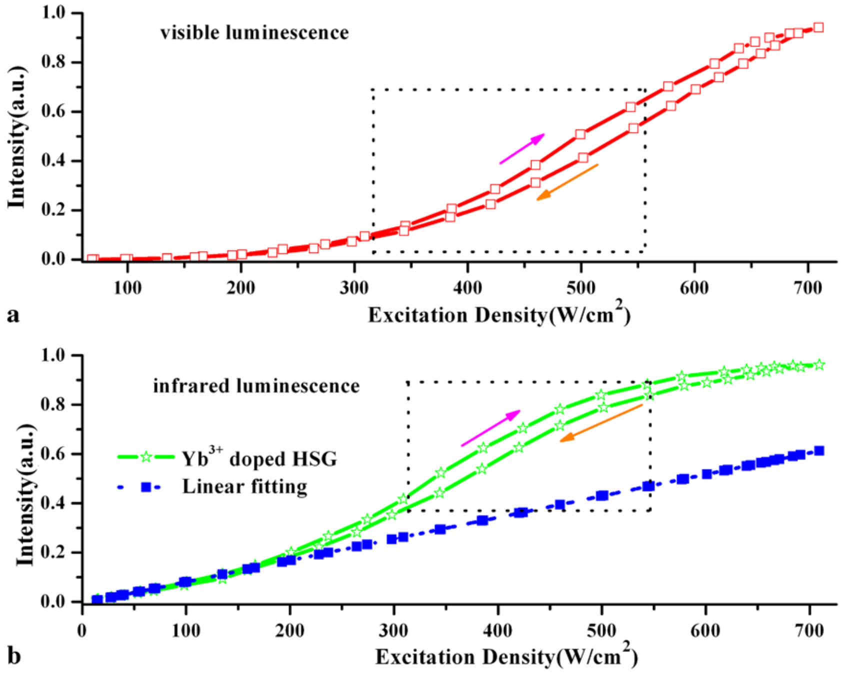

first investigated theoretically by Bowden and Sung and is caused by ground state, near dipole-dipole interaction [13]. In the IOB process there is usually an obvious switch phenomenon at cryogenic temperature (typically <40 K) [14–19] or with an external cavity [20, 21]. When temperature increases, the switch phenomenon becomes a gradually increasing/decreasing process [14, 15] and in the present work, we unexpectedly and interestingly find that Yb^{3+} doped HSG shows the same process at room temperature without external cavity as shown in Fig. 4. The curve by linear fitting the initial several data of NIR luminescence is also drawn in Fig. 4(b) (blue, dotted). We can see that the luminescence intensity in the NIR range is greatly enhanced and the relation between NIR intensity and laser power deviates linearly seriously, which would enlarge the slopes of the Yb^{3+} doped and Tb^{3+}/Yb^{3+} codoped HSGes. So the IOB phenomenon induces the abnormal UCL in Yb^{3+} doped and Tb^{3+}/Yb^{3+} codoped HSGes. The concentrations of Yb^{3+} and Tb^{3+} in the high silica glasses are $6 \times 10^{19}/\text{cm}^3$ and $1 \times 10^{19}/\text{cm}^3$ respectively. This concentration is consistent with that in $CsCdBr_3 : 1\%Yb^{3+}$ ($5.8 \times 10^{19}/\text{cm}^3$) [14] but much lower than that in $Cs_3Y_2Br_9 : 10Yb^{3+}$ ($3.9 \times 10^{20}/\text{cm}^3$) [15]. So in Yb^{3+} doped high silica glass the ion pairs responsible for IOB are isolated similar to that in $CsCdBr_3 : 1\%Yb^{3+}$. This can also be confirmed by the fact that both the NIR and VIS emission luminescence originating from the excited state increase when the excited state population increases as shown in Fig. 4, the same as that in $CsCdBr_3 : 1\%Yb^{3+}$ [14]. There are some remnant OH groups in the Yb^{3+} doped and Yb^{3+}/Tb^{3+} codoped high silica glasses, even though they are obtained by being sintered at 1200°C. OH groups may affect the fluorescence properties particularly when the laser power is high; the structure of glasses may also be altered due to the relatively high power laser. We measure the fluorescence spectra of the same sample under the same condition twice and the same results are obtained. Then we can confirm that the OH groups are not affected by the high power laser. What is more, high silica glass has a large heat transfer coefficient, comparable with that of silica glass, and the concentration of Yb^{3+} in high silica glass is low. So the influence of the laser on the structure of the high silica glass can also be eliminated.

We can see that the excitation density necessary for the observation of IOB is much lower than that in $CsCdBr_3 : 1\%Yb^{3+}$ and $Cs_3Y_2Br_9 : 10Yb^{3+}$. Usually the excitation density decreases when the temperature rises in the IOB process. So the low excitation density in Yb^{3+} doped HSG can be ascribed to the high temperature at which IOB is observed. IOB is caused by the near dipole-dipole interaction (NDD) between Yb^{3+} ions. Strong NDD is helpful to the observation of the IOB phenomenon. Shortening the Yb^{3+}–Yb^{3+} distance can enhance the NDD greatly. The Yb^{3+} ions are doped into porous glasses and then the Yb^{3+} doped porous glasses are sintered at high temperature (1200°C). If all the Yb^{3+} ions are monodispersed inside the high silica glass, the distance between each Yb^{3+} ions can be estimated by using $d = N^{1/3}$, where N is the concentration of Yb^{3+} ions. Then we can obtain the distance $d = 2.55$ nm, much larger than that in $CsCdBr_3 : 1\%Yb^{3+}$. If so, we can be sure that no IOB will be observed. Fortunately, we can say the negative of this assumption for the observation of obvious cooperative UCL from Yb^{3+} pair. When Yb^{3+} ions are doped into porous glass, they mainly stay on the surface of the channels inside the porous glass. In the sintering process, Yb^{3+} ions cluster and form pairs. The channels with thickness about several nanometers collapse and isolate the Yb^{3+} pairs after being sintered. So high Yb^{3+} pair formation can be realized in the Yb^{3+} doped high silica glass even though the concentration of Yb^{3+} is low. What is more, the radius of (Na^+, B^{3+}, Ca^{2+}, Si^{4+}) and O^{2-} is much smaller than that of (Cs^+, Y^{3+}, Cd^{2+}) and Br^-, so we can assume that the distance between the paired Yb^{3+} ions is much smaller than that in $CsCdBr_3 : 1\%Yb^{3+}$ or $Cs_3Y_2Br_9 : 10Yb^{3+}$. This induces the IOB phenomenon in Yb^{3+} doped HSG even at room temperature.

4 Conclusion

Yb^{3+} doped and Tb^{3+}/Yb^{3+} codoped HSG are prepared by an immersing and sintering method. The UCL properties under the excitation of 980 nm LD are investigated and the UCL process shows abnormal phenomena. The luminescence intensities of Yb^{3+} doped HSG versus laser power in VIS/NIR range are measured and both luminescence intensities show hysteretic behavior when the laser power is increased and decreased successively. This behavior is ascribed to the IOB of Yb^{3+} ions in HSG, which induces the abnormal UCL properties of Yb^{3+} doped and Tb^{3+}/Yb^{3+} codoped HSG.

Acknowledgements This work was financially supported by the National Natural Science Foundation of China (Grants 60878043 and No. 6070701).

References

1. I.R. Martín, A.C. Yanes, J. Méndez-Ramos, M.E. Torres, V.D. Rodríguez, J. Appl. Phys. **89**, 2520 (2001)
2. L. Feng, J. Zhang, J. Wang, H. Liang, Q. Su, Spectrochim. Acta Part A **67**, 886 (2007)
3. T. Yamashita, Y. Arai, T. Suzuki, Y. Ohishi, Proc. SPIE **6775**, 66750V (2007)
4. G.M. Salley, R. Valiente, H.U. Güdel, Phys. Rev. B **67**, 134111 (2003)
5. Y. Arai, T. Yamashita, S. Horiguchi, T. Suzuki, Y. Ohishi, Proc. SPIE **6890**, 689003 (2008)
6. T. Yamashita, Y. Ohishi, Proc. SPIE **6389**, 638912 (2006)
7. L. Huang, G. Qin, Y. Arai, R. Jose, T. Suzuki, Y. Ohishi, T. Yamashita, Y. Akimoto, J. Appl. Phys. **102**, 093056 (2007)
8. P.V. dos Santos, M.V.D. Vermelho, E.A. Gouveia, M.T. de Araujo, A.S. Gouveia-Neto, F.C. Cassanjes, S.J.L. Ribeiro, Y. Messaddeq, J. Chem. Phys. **116**, 6772 (2002)
9. X. Wang, S. Xiao, X. Yang, J.W. Ding, J. Mater. Sci. **43**, 1354 (2008)
10. E. de la Rosa, D. Solis, L.A. Diaz-Torres, P. Salas, C. Angeles-Chavez, O. Meza, J. Appl. Phys. **104**, 103508 (2008)
11. G.S. Maciel, A. Biswas, R. Kapoor, P.N. Prasad, Appl. Phys. Lett. **76**, 1978 (2000)
12. A.K. Kir'yanov, Y.O. Barmenkov, I.L. Martinez, A.S. Kurkov, E.M. Dianov, Opt. Express **14**, 3981 (2006)
13. C.M. Bowden, C.C. Sung, Phys. Rev. A **19**, 2392 (1979)
14. M.P. Hehlen, A. Kuditcher, S.C. Rand, S.R. Lüthi, Phys. Rev. Lett. **82**, 3050 (1999)
15. M.P. Hehlen, H.U. Gudel, Q. Shu, S.C. Rand, J. Chem. Phys. **104**, 1232 (1995)
16. M.P. Hehlen, H.U. Gudel, Q. Shu, S. Rai, S.C. Rand, Phys. Rev. Lett. **73**, 1103 (1994)
17. M.O. Ramírez, L.E. Bausá, J. Lumin. **102–103**, 206 (2003)
18. J.M. Ward, D.G. O'Shea, B.J. Shortt, S.N. Chormaic, J. Appl. Phys. **102**, 023104 (2007)
19. M.O. Ramirez, L.E. Bausa, A. Speghini, M. Bettinelli, L. Ivleva, J. Garcia Sole, Phys. Rev. B **73**, 035119 (2006)
20. J.M. Ward, D.G. O'Shea, B.J. Shortt, S.N. Chormaic, J. Appl. Phys. **102**, 023104 (2007)
21. A. Kuditcher, M.P. Hehlen, C.M. Florea, K.W. Winick, S.C. Rand, Phys. Rev. Lett. **84**, 1898 (2000)